Design of a novel TIR lens for optimizing the optical performance of white LED lamps

ANH Q. D. NGUYEN[a], P. X. LE[b], H. Y. LEE[c,*]
[a]*Nguyen Tat Thanh University, Ho Chi Minh, Vietnam*
[b]*Faculty of Electrical and Electronics Engineering, HCMC University of Food Industry, Ho Chi Minh, Vietnam*
[c]*Department of Electrical Engineering, National Kaohsiung University of Applied Sciences, Kaohsiung, Taiwan*

A novel TIR lens is proposed for optimizing the optical performance of white LED packages. The delineation of a novel TIR lens, including multi-curve collimator and multi-shape surface is determined by the Snell's law, the energy conservation law and the Monte Carlo ray tracking method. It is demonstrated that an optical efficiency of 95.69% under a beam angle of 30 degrees is accomplished by experiments. Furthermore, the illumination homogeneity increases to 0.195 in comparison with the commercial TIR lens uniformity of 0.032. The production cost of this novel lens should be low because it has no a reflector.

(Received October 12, 2017; accepted August 9, 2018)

Keywords: LED lighting, Optics design, Illumination homogeneity

1. Introduction

In recent years, remarkable efforts have been expended to develop white LEDs applications, which are regarded as the most promising illumination method to replace traditional lighting sources due to their superior features, such as low power consumption, high efficiency, and long life [1-5]. For this reason it is really important to provide a solution which increases quality and cuts prices of LED lights [6-8]. Besides, LED lamps usually cannot provide uniform illumination [9-12]. To deal with this problem, they need auxiliary devices for enhancing illumination homogeneity and luminous efficiency. As well, the intensity distribution curves of LED lamps can be adjusted according to manufacturing requirements. The TIR lens is acknowledged as a very useful auxiliary device for optimizing optical performance [13-15]. However, if the lens boundary cannot make an effort into total internal reflection, TIR lens would not efficiently reflect the incident light [16]. Therefore, TIR lens wants to be created with higher efficiency, it must be used a white holder to surround the conventional TIR lens, which helps the lost light collect but that makes the production cost higher. This is the fundamental reason why freeform lenses are difficult to apply in LED general lighting fields, widely [17-22]. The authors of the cited studies mostly concentrated on the productivity of TIR lenses but did not refer to applicability or mass production [23-28].

In this study, we propose an LED spot light equipped with a novel TIR lens without reflector to hold cost down but still increase optical efficiency. The novel TIR lens is generated from the combination of two elements, multi-curve collimator (MCC) and multi-shape surface (MSS), which can redistribute most of the incident rays. The design target is to produce a Lambertian white light LED having a beam angle of 30 degrees and a luminous efficiency of more than 95% and an illumination homogeneity higher than 0.032. The design process of the novel TIR lens includes two steps: 1) MCC designing; 2) MSS designing. Compared with commercial TIR lenses, the proposed TIR lens has better optical efficiency and higher illumination uniformity in the same LED source package. Moreover, the light intensity distribution easily meets the design requirement. In summary, this novel TIR lens is proposed for widespread use in LED lamps and to lower production costs.

2. Problem statement

The basic optical elements of an LED package include the primary and secondary optics elements. Although the LED module's performance greatly depends on the technology of primary optics elements, secondary optics elements are also very important for white LEDs technology to achieve higher quality. The light intensity distribution and the illumination homogeneity of an LED package can be adjusted based on the secondary elements. The radiations should be redistributed by the secondary elements to meet the demand of design.

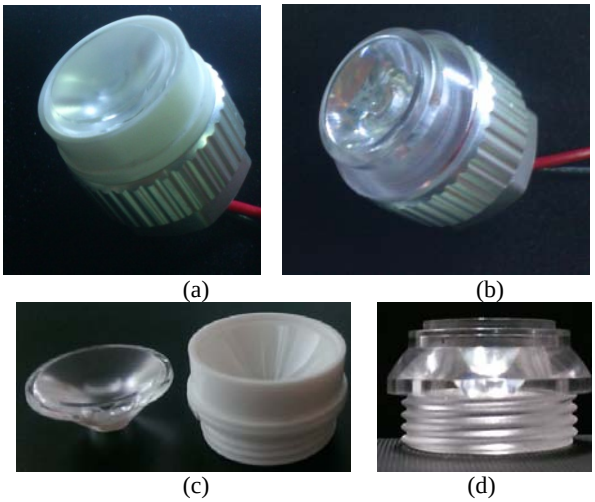

Fig. 1. The white LED package with: (a) Commercial sample I and its lens (c), (b) Commercial sample II and its lens (d)

In general, commercial secondary lenses with reflectors are used in LED packaging modules, such as those shown in Fig. 1 (a) and Fig. 1 (b). In sample I, the reflector is utilized to fix the lens and acts as a holder, as displayed in Fig. 1 (c). Sample II is a prism-shape lens which is used for total internal reflection (TIR) at the surfaces rather than for dispersion, as shown in Fig. 1 (d). However, the light rays such as yellow and blue light rays are refracted in different directions after passing through the surface of sample II. The non-optimized structure causes unexpected phenomena such as the yellow ring. Therefore, it makes eyes uncomfortable [7]. Consequently, the design idea of a novel TIR lens without reflector is proposed to reduce the production cost. This lens includes two main parts, which are the collimator and the micro-lens plane. The main objective of the TIR lens is to adjust incident light which is emitted from the light source to the micro-lens surface where the light rays will be redirected.

3. Principles of design

3.1. Design of collimator surface with three curves

In the MCC design process, the center of the LED source is set as the origin of a Cartesian coordinate system. A ray is traced from the origin to a corresponding point *P* on the optical surface. The law of refraction decides the relation of the light direction vector *I*, the optical surface normal vector *N*, and the outgoing light direction vector *O*, which are shown in Fig. 2. Based on the relation, through Monte Carlo ray tracing in computers, the generatrix *f(x)* of the TIR lens can be solved [8, 9] and the normal vector *N* can be obtained by Equation (1):

$$N = \frac{I - O}{|I - O|} \quad (1)$$

The 2D structure of the MCC consists of three curves, and each curve is an arc having its own curvature as shown in Fig. 2. The first curve, which is the largest extending angle and the shortest arc length as well as the smallest arc radius, has the most influence on the path of light because it is close to the LED light source. Contrarily, the third curve, which is the longest arc length and largest arc radius, has the smallest extending angle.

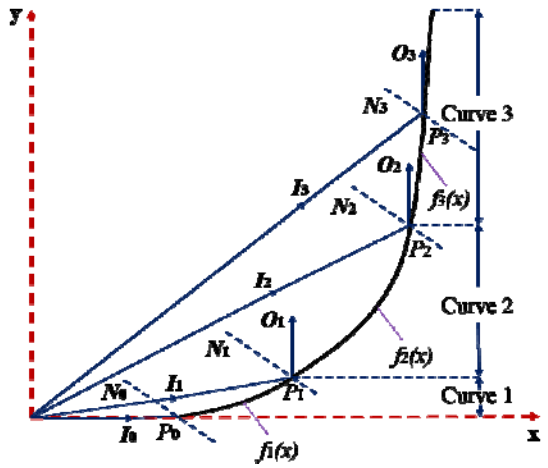

Fig. 2. Illustration of MCC designing

Actually, the objective of this MCC surface is to redirect the incident light into vertical direction, so this can be achieved by just one curve. However, to control light direction more easily, the generatrices of the MCC can be divided into three curves which correspond with the $f_1(x)$, $f_2(x)$ and $f_3(x)$ functions. These functions can be adjusted to redirect light rays which emit from an LED source. As a result, the light rays will be controlled to produce the required spotlight angle of 30 degrees.

Next, we can calculate the dispersion points of three functions. The P_0 point of the generatrix is set as the start point to find vector N_0. The vectors I_1, I_2, I_3 and the vectors N_1, N_2, N_3 intersect at P_1, P_2, P_3 points, in turn. This work is iterated until all the *P* points are discovered, so that the 2D curves of the $f_1(x)$, $f_2(x)$ and $f_3(x)$ functions can be constructed respectively by using SolidWorks and TracePro softwares. After that, through rotating the 2D contour about the optical axis, the axis symmetrical 3D MCC surface can be obtained. The below and above radii as well as the height of the MCC are 2.53 mm, 11.65 mm and 10.73 mm, in turn. Moreover, the cylindrical holder, with the thickness 0.35 mm, replaces the reflector. By adjusting the functions, the contour of MCC can be accomplished. MCC can replace absolutely the reflector of the sample I. The light direction can be controlled easily for designing TIR curves and adjusting light in the direction of MSS.

3.2. Design of optical surface with micro-lenses

Using Monte Carlo simulation, we investigate the schematic ray path of the LED package, as displayed in Fig. 3(a). Its result testifies that the illumination distribution on the surface is non-uniform. The light from the LED source excessively concentrates on two areas of the secondary lens plane, called the correction areas as shown in Fig. 3(b).

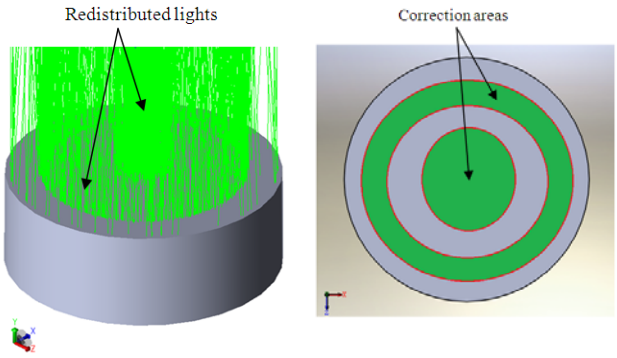

(a) (b)

Fig. 3. (a) The schematic ray path from sample I; (b) The top view picture for the correction areas having the unequal illumination at the center area and the outside area

The light rays should be redirected after passing the areas, which results in reducing the unequal illumination of the center area and the outside area. The correction area is the salient feature of MSS, which is composed of dome-like micro-lenses with different densities. The density is designed to be proportional to the output light energy reaching the light exit of the MCC, resulting in homogenizing the light illumination on the target plane. According to the energy conservation law, the light power on the target surface can be denoted as [10]:

$$\iint_{A} E_f \, ds = \sum_{i=1}^{N} \iint_{C_i} E_i \, ds = E_{total} \qquad (2)$$

Here A is the homogeneous illumination area, E_f is the luminance, N is the totalling of the cells, C_i is the area of the cell, E_i is the luminance of the homogeneous collimated radiation passing through the cell C_i, E_{total} is the total energy from the source. It means that the smaller number of cells used, the more homogeneity of illumination there is. Therefore, the density of micro-lenses in the high light energy areas is higher than that of the other areas. Correspondingly, the redirection of light in the high light density areas is significant, but not in other areas. This results in more homogeneous illumination compared to commercial lenses.

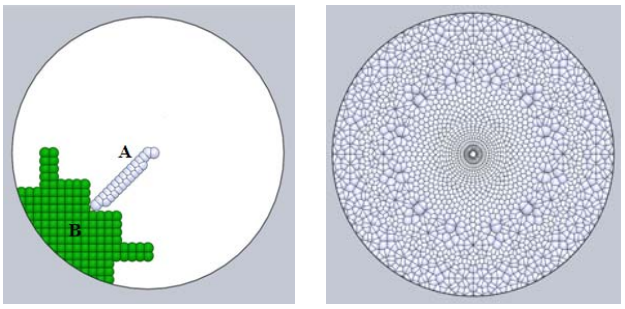

(a) (b)

Fig. 4. (a) Illustration of A and B matrices; (b) MSS designing

The original radius and the height of the dome shape micro-lens are in turn set as 0.5 millimeter and 0.17 millimeter. Two continuous peaks of the micro-lens have a length of 0.5 millimeter. The MSS includes the micro-lens matrices A (silver) and B (green) as presented in Fig. 4 (a). The matrices are arrayed many times around the original MSS to establish the complete MSS. The more the micro-lens matrices, the better the illumination uniformity achieved. However, the production cost increases over time. Besides, the luminous efficiency can reduce as increasing the micro-lens matrices. Accordingly, the balance of illumination homogeneity, luminous efficiency and production cost is an important task. After computing, this study proposed the matrices A and B should be respectively overlapped 40 and 12 times, as displayed in Fig. 4(b).

4. Optical simulations

The optical simulation is performed by the assistance of the TracePro program. The main work includes: 1) Building the LED packaging with proper optical properties; 2) Simulating two commercial secondary lenses (sample I and sample II) and analyzing their performance; 3) Designing a novel TIR lens to improve the performance of an LED lamp.

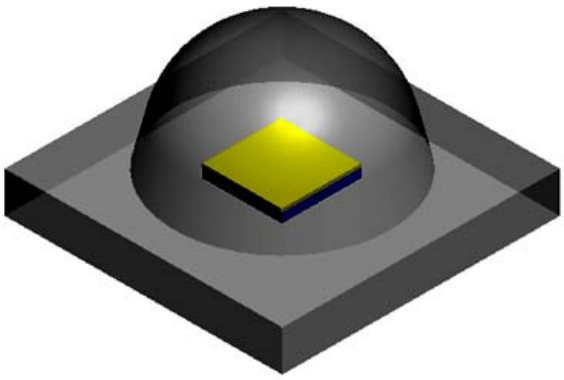

Fig. 5. Simulated white LED package

A 3-D LED source package was built, as displayed in Fig. 5. The dimensions of blue LED chip are 1 mm x 1 mm (base) and 0.15 mm (height). The chip was covered by the YAG:Ce^{3+} phosphor layer with a 0.05 mm thickness. Moreover, the optical parameters of YAG:Ce^{3+} for Monte Carlo simulation such as absorption, scattering, and anisotropy coefficients should be provided in Table 1.

The luminous power of each blue chip is 1 W with the peak wavelength of 455 nm. In our experiments, the polymethyl methacrylate (PMMA) material was selected for manufacturing the novel sample. After constructing the white LED package and two commercial lenses, Monte Carlo simulations were applied to verify the illumination uniformity and the light intensity distribution.

Table 1. Optical properties of LED packaging materials

	Refra. index	Absor. coeff. (/mm)	Scatt. coeff. (/mm)	Aniso. coeff.
YAG:Ce^{3+}	1.83	1.5	5	0.9
p-GaN	2.43	8	--	--
n-GaN	2.39	8	--	--
MQW	2.5	8	--	--
Lens	1.586	--	--	--
Silicone glue	1.54	--	--	--

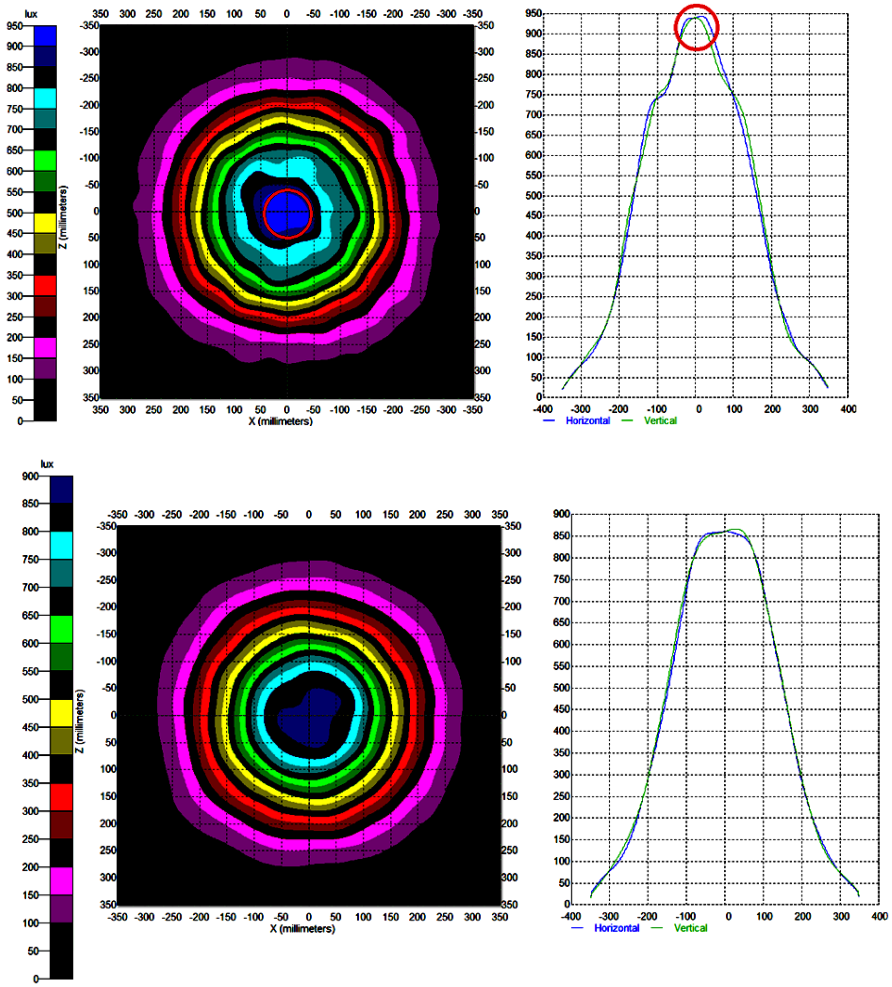

Fig. 6. The illumination map and its distribution without MSS (above) and with MSS (below)

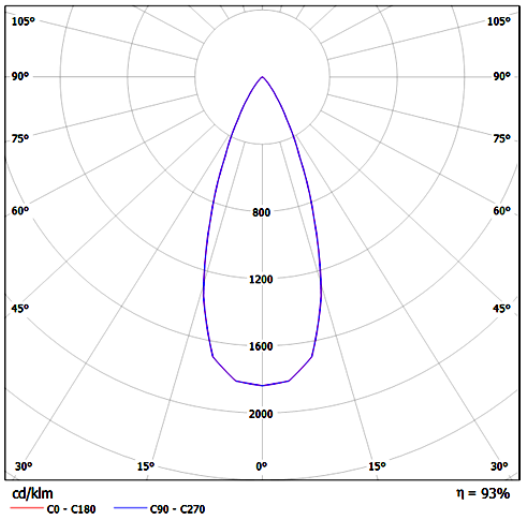

Fig. 7. The simulated intensity distribution of the proposed TIR lens with the beam angle of 30 degrees

Fig. 6 displays the illumination map on a target surface 500 mm away, which indicates that the light spot size is about 350 mm in radius. According to the simulation results, the peak illumination can be reduced from about 950 lux (on red ring) to near 850 lux for these two lens structures. It means that the LED uniform illumination will be increased by using the proposed secondary lens. Meanwhile, the total efficiency of the proposed TIR lens and the spotlight angle achieve 93% and 30 degrees, in turn, as demonstrated in Fig. 7. In the computing processes, there are many factors which affect the output results such as the phosphor compound, and the LED chip. Therefore, we try to preserve parameters which are the same as the actual materials for achieving precise simulation results. In the next section, the detailed experimental results will be presented.

5. Experimental measurement

Making use of a Goniophotometer, the measurements of the light intensity distributions, the luminous flux and the optical efficiency of LED light modules are accomplished. The LED lamp's optical efficiency is described by the ratio of the luminous flux with TIR lens to the luminous flux without TIR lens. Illumination homogeneity is calculated by the ratio of the minimum illumination to the mean illumination. At 500 mm away from the source, a photometer is employed for measuring the illumination on the 700 mm^2 regions.

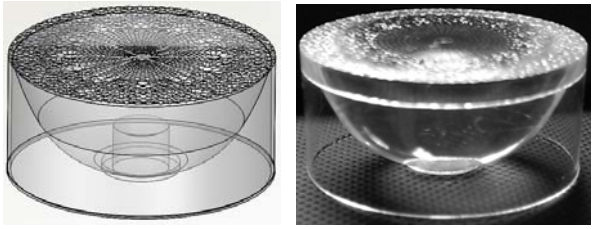

(a) (b)

Fig. 8. The novel TIR lens: (a) Simulation model and (b) Experiment model

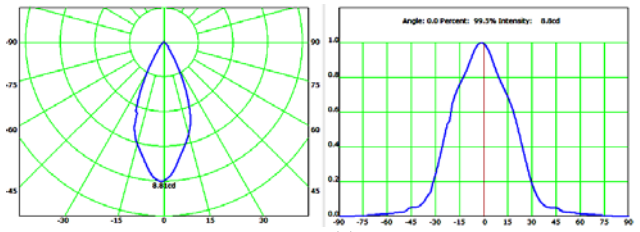

(a)

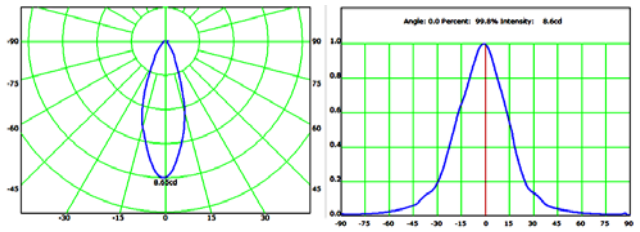

(b)

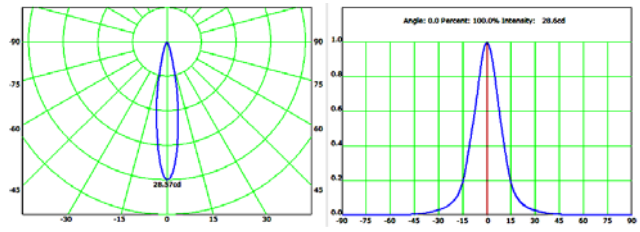

(c)

Fig. 9. The measured polar (left) and cartesian (right) intensity distribution curves of (a) sample I, (b) the proposed TIR lens with the beam angle of 30 degrees and (c) sample II

The proposed TIR lens is prototyped and shown in Fig. 8. The measured intensity distribution of the novel sample and the commercial samples are presented in Fig. 9. It indicates that the experimental and simulation results are alike with the beam angle of 30 degrees. The beam angle is the opening in degrees width at 50% of the

maximum intensity (or called spotlight angle). The performance of the proposed lens and the traditional ones are shown in Table 2.

Table 2. Comparisons of the luminous flux and the optical efficiency among the novel sample and the commercial samples

Samples	Luminous flux (lm)	Optical efficiency (%)
Sample I	117.9	95.85
Sample II	111.1	90.32
Novel sample	117.7	95.69

To evaluate the deviation between the simulated TIR lens model and the manufactured TIR lens sample, their angular intensity distributions are analyzed by using the normalized cross correlation (NCC). The NCC formula is shown in Eq. (3) as:

$$NCC = \frac{\sum_n [I(\theta_n)_e - \overline{I_e}][I(\theta_n)_s - \overline{I_s}]}{\sqrt{\sum_n [I(\theta_n)_e - \overline{I_e}]^2 \sum_n [I(\theta_n)_s - \overline{I_s}]^2}} \quad (3)$$

Here I_s and I_e are the simulated and real experimental values of the relative light intensity, respectively. θ_n is the *n*-th angular displacement, $\overline{I_s}$ and $\overline{I_e}$ are the mean values of simulations and optical measuring experiments accomplished by a goniophotometer across the angular range. The calculated NCC value is higher than 98.5%. It means that there is an insignificant effect of the processing deviation on the optical performance of freeform lens.

Based on our optical measurement, the optical efficiency of the novel lens and sample I are 95.69% and 95.85%, respectively. The light power and the optical efficiency of the novel TIR lens are 6.6 lm and 5.37% more than those of sample II, respectively. Moreover, the novel lens is accomplished without a reflector, resulting in reduction of production cost.

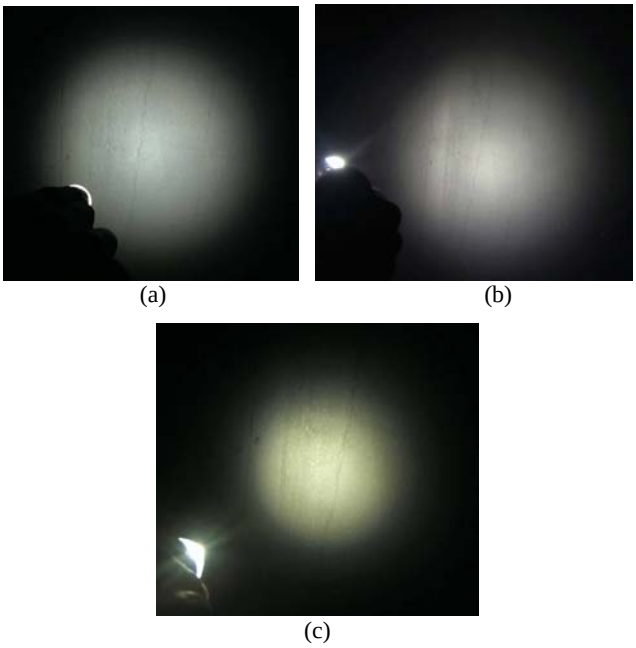

(a) (b) (c)

Fig. 10. Lighting performance of sample I (a), the proposed TIR lens (b) and sample II (c) at 500 mm away the 700 mm^2 areas

Fig. 10 shows the lighting performance of the novel sample and the commercial samples. It can be observed that the white light distribution of the proposed TIR lens is better than that of sample II which has a significant yellow ring phenomenon. Meanwhile, it is almost equivalent to the white light distribution of sample I. This indicates that the novel TIR lens can provide better white light uniformity.

Referring to the experimental results in Table 3, measured by lux meter, it can be concluded that enhancements of illumination uniformity can be made. For a target surface of 700 mm^2, the illumination homogeneity is increased to 0.096 and 0.163 in comparison with sample I and sample II, in turn.

Table 3. Comparisons of the illumination homogeneity among the novel sample and the commercial samples

Samples	Target plane	Average illumination	Minimum illumination	Uniformity	Enhanced uniformity
Sample I	700 mm^2	270.57 lux	26.8 lux	0.099	0
Sample II	700 mm^2	242.74 lux	7.8 lux	0.032	0
Novel sample	700 mm^2	259.5 lux	50.5 lux	0.195	0.096 (@ I) 0.163 (@ II)

(@ = compared with each sample)

6. Conclusions

In this paper, a novel TIR lens design with MCC and MSS is proposed. Both MCC and MSS redirect the light rays according to the design requirements, which results in achieving better optical performance and lower production cost. The LED performance with the proposed TIR lens is better than that of the two commercial lenses. The simulation results show the novel TIR lens having optical efficiency of 93% with a beam angle 30 degrees. Meanwhile, the experimental results show its efficiency of 95.69% with the same angle distribution. With the novel TIR lens, the illumination homogeneity of 0.195 is higher than that of the commercial TIR lenses.

Acknowledgements

This research is funded by Foundation for Science and Technology Development Nguyen Tat Thanh University.

References

[1] N. D. Q. Anh, M. -F. Lai, H. -Y. Ma, H. Y. –Lee, J. Chin. Ins. Eng. **38,** 297 (2015).
[2] M. -F. Lai, N. D. Q. Anh, H. -Y. Ma, H. -Y. Lee, J. Chin. Ins. Eng. **39,** 468 (2016).
[3] J. -J. Chen, T. -Y. Wang, K. -L. Huang, T. -S. Liu, M. D. Tsai, C. -T. Lin, Opt. Express **20,** 10984 (2012).
[4] K. Wang, D. Wu, Z. Qin, F. Chen, X. B. Luo, S. Liu, Opt. Express **19,** A830 (2011).
[5] Z. R. Zhen, H. Xiang, L. Xu, Appl. Opt. **48,** 6627 (2009).
[6] Y. Ding, X. Liu, Z. -R. Zheng, P. -F. Gu, Opt. Express **16,** 12958 (2008).
[7] Z. Liu, S. Liu, K. Wang, X. Luo, International Conference on Electronic Packaging Technology & High Density Packaging 2008, Shanghai, China, p. 1–8.
[8] R. Winston, J. C. Miñano, P. Benítez, eds., with contributions by N. Shatz and J. C. Bortz, eds. Nonimaging Optics, Elsevier (2005).
[9] L. Sun, S. Z. Jin, S. Y. Cen, International Conference on Communications and Photonics Conference and Exhibition 2009, Piscataway, New Jersey, p. 1–10.
[10] H.-W. Lee, B. -S. Lin, Opt. Express **20**, A788 (2012).
[11] A. Teupner, K. Bergenek, R. Wirth, P. Benítez, Juan Carlos Miñano, Opt. Express **23**, A118 (2015).
[12] F. Pijlman, Imaging and Applied Optics 2015, Arlington, Virginia United States, p. FM2B.2.
[13] D. H. Liu, X. H. Zhang, S. Zhang, J. Opt. Soc. Korea **20**, 739 (2016).
[14] D. L. Ma, Renewable Energy and the Environment, Freeform Optics 2013, Tucson, Arizona United States, p. FT2B.1.
[15] Chung-Yu Tsai, J. Opt. Soc. Am. A **33**, 785 (2016).
[16] C. Chen, X. H. Zhang, J. Opt. Soc. Am. A **31**, 1118 (2014).
[17] X.-H. Lee, I. Moreno, C.-C. Sun, Opt. Express **21**, 10612 (2013).
[18] B. –J. Chen, Y. –T. Chen, I. Ullah, C. –H. Chou, K. –C. Chan, Y. –L. Lai, C. –M. Lin, C. –M. Chang, A. J. W. Whang, Appl. Opt. **54**, E165 (2015).
[19] Z. T. Li, S. D. Yu, L. W. Lin, Y. Tang, X. R. Ding, W. Yuan, B. H. Yu, Appl. Opt. **55**, 10375 (2016).
[20] R. M. Wu, C. Y. Huang, X. Y. Zhu, H. –N. Cheng, R. G. Liang, Optica **3**, 840 (2016).
[21] C. Bösel, N. G. Worku, H. Gross, Appl. Opt. **56**, 3679 (2017).
[22] S. X. Hu, K. Du, T. Mei, L. Wan, N. Zhu, Opt. Express **23**, 20350 (2015).
[23] Z. Feng, B. D. Froese, R. G. Liang, Appl. Opt. **55**, 4310 (2016).
[24] S. Zhao, K. Wang, F. Chen, D. Wu, S. Liu, J. Opt. Soc. Am. A **28**, 815 (2011).
[25] X. F. Wu, G. F Jin, J. Zhu, Appl. Opt. **56**, 2405 (2017).
[26] R. J. Lin, M. –S. Tsai, C. –C. Sun, Opt. Express **23**, 16715 (2015).
[27] L. Hongtao, C. Shichao, H. Yanjun, L. Yi, Opt. Express **21**, 1258 (2013).
[28] J. Yu, Z. J. Qiu, F. Z Fang, Appl. Opt. **53**, 4914 (2014).

*Corresponding author: leehy@mail.ee.kuas.edu.tw